Available online at www.sciencedirect.com
ScienceDirect
International Journal of Heat and Mass Transfer 51 (2008) 186–197
International Journal of HEAT and MASS TRANSFER
www.elsevier.com/locate/ijhmt

Numerical analysis of blast furnace hearth inner profile by using CFD and heat transfer model for different time periods

Yu Zhang [a], Rohit Deshpande [a], D. (Frank) Huang [b], Pinakin Chaubal [b], Chenn Q. Zhou [a,*]

[a] Department of Mechanical Engineering, Purdue University Calumet, Hammond, IN 46321, USA
[b] Mittal Steel Company, USA R&D Center, East Chicago, IN 46312, USA

Received 15 January 2007; received in revised form 6 April 2007
Available online 13 August 2007

Abstract

The campaign life of a modern blast furnace is determined by the residual thickness of the refractory in the hearth. A new methodology is established to predict the inner profile of a blast furnace during operation. This methodology combines 3-D CFD model, which is used to predict the hot face temperature for a given inner profile, and a 1-D heat transfer model, which is used to predict and fine tune the inner profile. The effectiveness of this methodology has been demonstrated by its application to one blast furnace with good agreement between predicted and measured temperatures.

Keywords: CFD; Iron making; Heat transfer; Blast furnace hearth; Erosion; Skull

1. Introduction

The blast furnace is the main industrial unit for iron-making. A longer campaign life can significantly lower the costs for production and increase productivity by reducing the downtime and capital costs for the relines. A crucial region of the furnace is its hearth located at its bottom in which the liquid iron and slag are collected and tapped out. The life span of a blast furnace is mainly determined by the residual thickness of the refractory lining in the hearth which depends on progress of the hearth lining erosion. The hearth lining erosion is significantly affected by the hot metal flow patterns and heat transfer through the refractory which are dependent on the furnace operating conditions. To extend the blast furnace campaign life, it is important to adjust operating conditions to reduce the hearth lining erosion [1]. Therefore, it is critical to monitor the hearth refractory thickness and the inner profile [2,3]. The inner profile is defined by the hot face profile of the hearth lining and hearth skull if it is formed on the hearth lining. In the other words, the inner profile is the profile of the interface between the liquid phase and the solid side wall and bottom which may be the refractory lining or the hearth skull. The inner profile changes over time due to the erosion or skull build-up.

Due to the difficulty in making measurements inside the hearth, novel approaches to predict the inner profile of a hearth is desired. Recently, with the advancement of computational technologies, efforts have been made to use computational fluid dynamics (CFD) modeling to elucidate the internal conditions of the blast furnace hearth. The mathematical modeling of hot metal flow and heat transfer in the blast furnace hearth started 20 years ago. In the early models, the flow inside the hearth was decoupled with the heat transfer in the refractories. A CFD model without conjugate heat transfer was developed to investigate the recirculatory flow induced by natural convection and its effect on dissolution of carbonaceous refractories into the melt [4]. It considered a situation where the taphole was plugged, and assumed the hearth to be coke free. A hearth erosion model was made by assuming that the erosion is caused by carbon dissolution only [5] and was validated using a 2-D water model. Tachimori [6] and Ohno et al. [7]

* Corresponding author. Tel.: +1 219 989 2665.
E-mail address: qzhou@calumet.purdue.edu (C.Q. Zhou).

0017-9310/$ - see front matter © 2007 Elsevier Ltd. All rights reserved.
doi:10.1016/j.ijheatmasstransfer.2007.04.052

Nomenclature

H_{flux}	measurement heat flux
K_{CB}	carbon brick thermal conductivity
K_{FB}	fire brick thermal conductivity
K_{skull}	skull thermal conductivity
R_{CB}	carbon brick thermal resistance
R_{FB}	fire brick thermal resistance
R_{skull}	skull thermal resistance
r_{CB}	carbon brick radius
r_{FB}	fire brick radius
r_{HF}	hot face radius
r_{skull}	skull radius
T_{CB}	interface temperature between fire brick and carbon brick
T_{FB}	interface temperature between fire brick and skull
T_{HF}	hot face temperature
$T_{d,f}$	CFD temperature at deep position
$T_{d,m}$	deep thermocouple measurement temperature
$T_{old,face}$	temperature at old hot face position
$T_{s,f}$	CFD temperature at shallow position
$T_{s,m}$	shallow thermocouple measurement temperature

undertook a pioneering effort to develop the relationship between hot metal flow and heat transfer in the hearth. Later, a model was developed and applied to analyze the hearth flow and the refractory heat transfer together using very coarse computational grids [8]. Recently, a CFD model was applied to a real commercial blast furnace for predicting the fluid flow pattern and temperature profiles in the hot metal and the hearth refractories using the general commercial CFD package CFX [9]. The model was evaluated using plant data and was used to conduct a series of parametric studies. Similar studies were made to simulate the same blast furnace to predict the shear stress and heat flux on the wall using the FLUENT package [3]. In both simulations, however, the fixed temperature boundary conditions were specified on the side and bottom refractory walls and the computational domain was assumed symmetric [3,9].

For all the existing CFD models, the main focus has been on hot metal flow characteristics at different operating and geometric conditions. The estimation of the inner profile of a blast furnace hearth has reply on the calculations based on heat transfer through refractory and measure refractory temperatures [8,10–12]. A few attempts have been made to use CFD models to estimate the hearth inner profile [3,13] with a number of assumptions such as symmetrical geometry and given hot face temperature and hearth drainages.

Recently, a truly 3-D CFD model was developed to simulate the hot flows of hot metal and molten slag [14] in the hearth along with the detailed temperature distributions in the liquid phases and the wearing linings [15–20]. The detailed hearth temperature results showed that the temperatures of the hot face vary with the locations in a wide range rather than a uniform distribution assumed by other researchers. This finding implies that non-uniform hot face temperatures should be used for the estimation of the inner profile. The truly 3-D model has provided a valuable tool to investigate the flow patterns and heat transfer inside the hearth and refractory at different operating condition. It can, however, be used only for a given inner profile. In order to provide a more accurate and efficient method for predicting the erosion and inner profiles, a new methodology has been established for predicting the inner profile. The principle of this new methodology is using the 3-D CFD model to predict the hot face temperatures based on the give inner profile and using the 1-D heat transfer model to predict the hot face position according to the measured refractory temperatures and the material properties of the hearth except the corner areas. This methodology provides more accurate predictions by using real non-uniform hot face temperatures and saves the computer time significantly for the 3-D inner profile calculation, which makes it possible and practicable to predict the inner profile of a real blast furnace at different operating time periods. The details of the methodology and results are described in the following sections.

2. Methodology

Fig. 1a shows the hearth structure of the Inland Harbor (IH) No. 7 Blast Furnace of Mittal Steel USA. The hearth is occupied by hot metal (liquid iron and carbon alloy), molten slag, active coke bed, and deadman. The refractory of the hearth is lined with carbon blocks along with two layers of ceramic pads on the top of the hearth bottom. Initially, there is a protection layer, i.e., blow-in lining, of 114 mm thickness on the sidewall and the bottom of the hearth for the start-up of the new built blast furnace. During operation, the hearth lining will be eroded due to various mechanisms, such as chemical reaction between the brick and hot metal and molten slag, the alkali and zinc attack, and the thermal stresses, etc. On the other hand, the hearth skulls, mainly coke, slag and iron, may also build-up on the hot face of the hearth linings. The hearth lining erosion and the skull buildup are affected by flow and heat transfer conditions.

The 3-D CFD hearth model, which simulates the hot metal flow and temperature distributions inside a hearth as well as conjugate heat transfer through solid walls, can provide the temperatures at the hot face, which is also called the inner profile or the interface between the liquid and the hearth linings or the hearth skull [16]. However the hot face position, i.e. the inner profile needs be specified

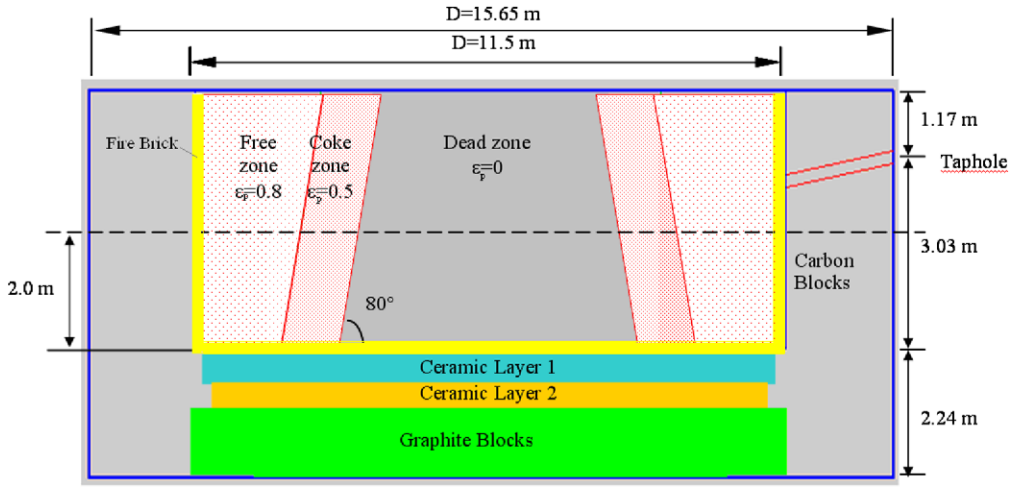

(a) Schematics of the Mittal IH 7 blast furnace hearth

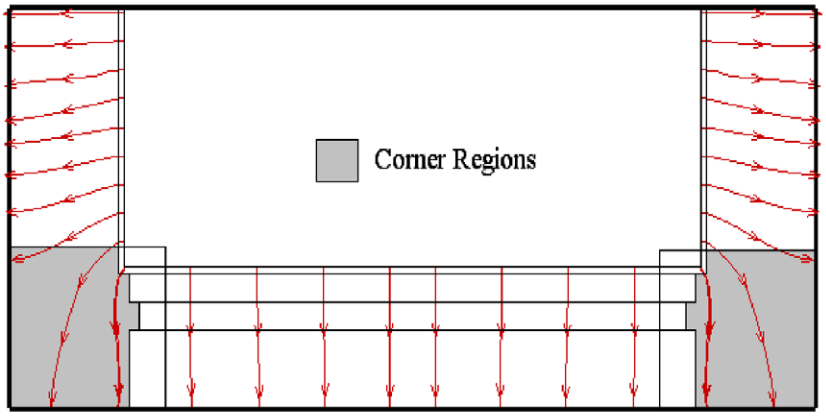

(b) Predicted heat flux paths in the plane at 90 degree to the taphole

Fig. 1. Blast furnace hearth.

as the internal boundary for the 3-D CFD hearth simulation. Theoretically, the 3-D inner profile can be adjusted in a proper way to make the computed temperature profiles exactly match the measured temperatures, however, it is very time consuming and almost impossible to predict the inner profile of a real blast furnace hearth on today's PC. Fortunately, as shown in Fig. 1b, the 3-D CFD simulations show that the heat flux paths through the linings of a hearth with sidewall and bottom cooling are the "1-D" straight lines in the most area except the taphole and the corner areas. This fact make it possible to predict the inner profile through the "1-D" (cylindrically) inverse heat transfer calculation based on the hot face temperatures and refractory temperatures measured near the cold end of the hearth linings for the most area. The inner profile in taphole and corner areas is adjusted separately.

The detailed procedure of this new methodology is illustrated in Fig. 2 and described in the following:

1. Use the 3-D CFD heath model to calculate hot metal flow and the temperature distributions in the hearth and determine the hot face temperature based on a given inner profile.
2. Apply the 1-D inverse heat transfer calculation to modify the interface position and get a new inner profile for the area other than the corners based on the hot face temperatures obtained in step 1.
3. Repeat steps 1 and 2 until the hot face temperatures are converged.
4. Fine tune the inner profile until the CFD predicted temperatures match the temperatures measured by all the thermocouples.

This methodology can be used to predict the inner profile of a blast furnace hearth accurately and efficiently.

3. 3-D CFD model

The 3-D CFD model solves the governing equations of the flow properties and heat transfer on a computational grid with specified boundary and initial conditions [16,17]. As shown in Fig. 1a, the calculation domain is divided by different zones [17], i.e., the free zone, coke zone, dead zone, carbon brick zone, ceramic pads, and fire brick zone (blow-in lining). The deadman position, which may sit on the hearth floor or float in the hot metal, can be

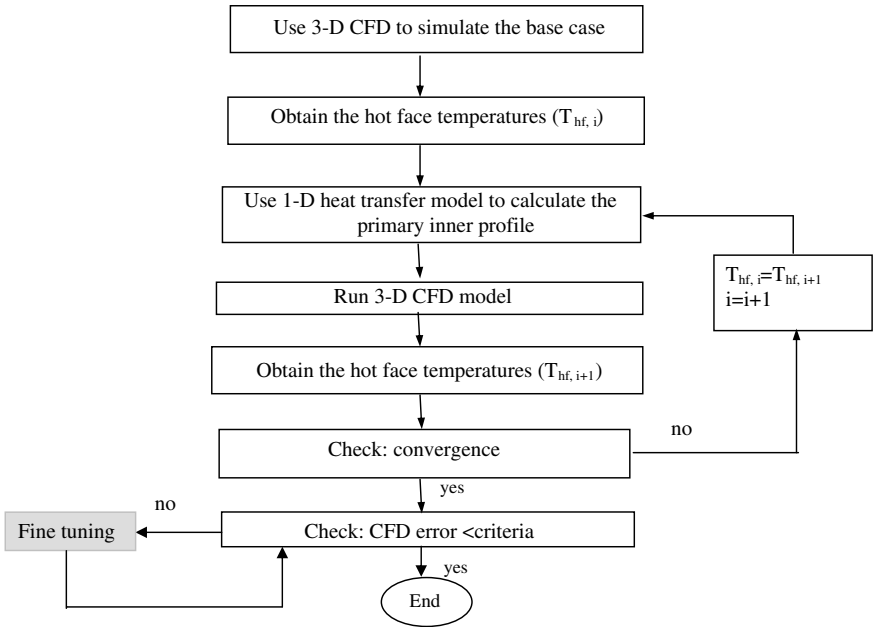

Fig. 2. Methodology for predicting the erosion and inner profile of the hearth.

predicted using the temperatures measured by the thermocouples embedded at the hearth bottom lining. In this study, it is assumed that the deadman is sitting on the bottom of the hearth. The deadman is porous based on the industrial observations [1], however most of the pores are not permeable to the liquid because they are closed or opened at only a single side. Those pores are opened at least on two sides and allow liquid flow through them are denoted as permeable pores and their volume fraction is named as permeable porosity. Different zones have different permeable porosity (ε_p). For the free zone, the permeable porosity is given as 0.8, the coke zone porosity is assumed as 0.5, and the dead zone is not permeable to the liquid. This assumption is based on the industrial observations [1]. All the hearth linings are designed and constructed as not permeable to the hot metal.

In the CFD simulations, the hearth is considered to be at steady state with a given hot metal flow rate. The free surface of the hot metal is assumed flat and horizontal. Conjugate heat transfer is included. Natural convection is not considered in the momentum equation. The governing equations of flow properties are derived from fundamental conservation laws and relevant state relations. The equations of mass, momentum, enthalpy are all elliptic partial differential equations. For convenience in numerical formulation, these equations are presented in the common form as Eq. (1).

$$\sum_{i=1}^{3} \frac{\partial}{\partial x_i}\left(\rho u_i \xi - \Gamma_\xi \frac{\partial \xi}{\partial x_i}\right) = S_\xi \tag{1}$$

where ξ is a general flow property, x_i, $i = 1,3$ are coordinates, u_i, $i = 1,3$ are velocity components, Γ is effective diffusivity, and S_ξ is the sum of source terms. For the region

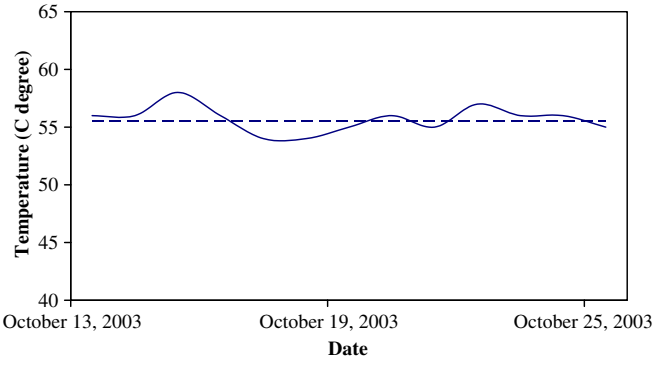

Fig. 3. An example of the temperature history recorded by a thermocouple.

with permeable porosity permeability between 0 and 1, the special treatment of the porous medium in the governing equations can be found in the previous publication [16]. In the dead zone, since the permeable porosity is zero, the velocity in this region is zero.

The hearth lining erosion process is very slow. It can be predicted weekly or monthly even periodically according the hearth temperature changes. Fig. 3 shows an example of the hearth sidewall temperatures in the first simulation period measured by a thermocouple which is embedded near the cold face of the carbon bricks.

4. 1-D Heat transfer model

Inverse heat transfer models are widely applied to solve different industrial problems. Huang et al. developed a method to predict the heat flux distributions in cutting tools [21]. Hills et al. used 1-D inverse heat transfer calcu-

lation to estimate the surface temperature and heat flux from temperature measurements at subsurface locations [22]. Dai et al. applied inverse heat transfer method to analyze the solid-layer growth from melt crystallization [23]. In this paper a special 1-D inverse heat transfer model is developed to estimate the inner profile of the hearth in combination with a 3-D CFD model.

Based on 3-D CFD simulation results, heat transfer through the side and bottom walls can be assumed as one-dimensional in most areas. With this assumption, a one-dimensional Fourier's Law in cylindrical coordinate system is used to estimate the refractory and skull thickness in the hearth. Fig. 4 shows the side wall structures at different situations. In general, the side wall is composed of three materials or layers which are the carbon brick (CB), fire brick (FB), and skull. T_{HF} and r_{HF} are the temperature and radius of the hot face, respectively. In addition, $T_{s,m}$ is the shallow thermocouple temperature, which is located near the shell, and $T_{d,m}$ is the deep thermocouple temperature, which is in farther distance from the shell. The one-dimensional steady-state Fourier's Law in cylindrical coordinates, with no heat generation, is shown in Eq. (2). The one-dimensional steady-state Fourier's Law in cylindrical coordinates, with no heat generation, is shown in Eq. (2)

$$H = -kA\frac{dT}{dr}, \quad \text{where } A = 2\pi rL \tag{2}$$

The side wall structure can be divided up into four sections, q_1 thru q_4 as shown in Fig. 4a. The heat fluxes in each section can be calculated by Eqs. (3)–(6).

$$H_1 = \frac{2\pi L(T_{HF} - T_{FB})}{\frac{1}{k_{skull}}\ln\left(\frac{r_{FB}}{r_{HF}}\right)} \tag{3}$$

$$H_2 = \frac{2\pi L(T_{FB} - T_{CB})}{\frac{1}{k_{FB}}\ln\left(\frac{r_{CB}}{r_{FB}}\right)} \tag{4}$$

$$H_3 = \frac{2\pi L(T_{CB} - T_{d,m})}{\frac{1}{k_{CB}}\ln\left(\frac{r_D}{r_{CB}}\right)} \tag{5}$$

$$H_4 = \frac{2\pi L(T_{d,m} - T_{s,m})}{\frac{1}{k_{CB}}\ln\left(\frac{r_S}{r_D}\right)} \tag{6}$$

Based on the 1-D steady-state heat transfer model, the heat balance can be obtained as follows:

$$H_1 = H_2 = H_3 = H_4 \tag{7}$$

Solving above equations yields:

$$\frac{T_{HF} - T_{d,m}}{\frac{1}{k_{FB}}\ln\left(\frac{r_{CB}}{r_{HF}}\right) + \frac{1}{k_{CB}}\ln\left(\frac{r_D}{r_{CB}}\right) + \frac{1}{k_{skull}}\ln\left(\frac{r_{FB}}{r_{HF}}\right)} = \frac{T_{d,m} - T_{s,m}}{\frac{1}{k_{CB}}\ln\left(\frac{r_s}{r_D}\right)} \tag{8}$$

The hot face radius, r_{HF}, can be obtained by rearranging Eq. (8):

$$r_{HF} = \frac{r_{FB}}{\exp\left[\frac{(T_{HF}-T_{d,m})}{(T_{d,m}-T_{s,m})}\left(\frac{k_{skull}}{k_{CB}}\ln\left(\frac{r_S}{r_D}\right) - \frac{k_{skull}}{k_{FB}}\ln\left(\frac{r_{CB}}{r_{FB}}\right) - \frac{k_{skull}}{k_{CB}}\ln\left(\frac{r_D}{r_{CB}}\right)\right)\right]} \tag{9a}$$

Eq. (9a) gives the hot face radius when the skull is building up on the inner surface of firebrick as displayed in Fig. 4a. If the erosion happens inside the firebrick as shown in Fig. 5b, the hot face radius is calculated by Eq. (9b).

$$r_{HF} = \frac{r_{CB}}{\exp\left[\left(\frac{T_{HF}-T_{d,m}}{T_{d,m}-T_{s,m}}\right)\frac{k_{FB}}{k_{CB}}\ln\left(\frac{r_s}{r_D}\right) - \frac{k_{FB}}{k_{CB}}\ln\left(\frac{r_D}{r_{CB}}\right)\right]} \tag{9b}$$

If firebrick is totally gone due to erosion and skull is building up on the inner surface of carbon brick as shown in Fig. 5c, the hot face radius is calculated by Eq. (9c)

$$r_{HF} = \frac{r_{CB}}{\exp\left[\frac{(T_{HF}-T_{d,m})\left(\frac{1}{k_{CB}}\ln\left(\frac{r_S}{r_D}\right)\right)}{(T_{d,m}-T_{s,m})} - \frac{1}{k_{CB}}\ln\left(\frac{r_D}{r_{CB}}\right)k_{skull}\right]} \tag{9c}$$

If the carbon brick starts to be eroded as illustrated in Fig. 5d, the hot face radius is calculated by Eq. (9d).

$$r_{HF} = \frac{r_D}{\exp\left[\ln\left(\frac{r_S}{r_D}\right)\frac{T_{HF}-T_{d,m}}{T_{d,m}-T_{s,m}}\right]} \tag{9d}$$

In the simulations, all the 4 possible situations are considered and the proper equations are used to calculate the hot face positions in the side walls. The equations for the hot face calculations at the bottom are very similar to those in the side walls.

5. 1-D Fine tuning procedure

The hot face temperatures can be obtained after several iterations in the steps 1 and 2 as described in the methodology section. In order to adjust the hot face position more effectively, a fine tuning procedure is established based on the 1-D heat transfer model. Fig. 5 summarizes all different situations where the fine tuning procedure can be applied. Due to the space limitation, only one situation, which is illustrated in Fig. 6a, is described in the following. Based on the measured temperatures, the heat flux for a given location can be calculated by Eq. (10):

$$H_{flux} = \frac{T_{d,m} - T_{s,m}}{\frac{1}{K_{CB}}\left(\ln\left(\frac{r_s}{r_d}\right)\right)} \tag{10}$$

Assuming R^D_{Old} and R^D_{New} as the thermal resistance between the old and new hot face and the tip of the deep thermocouple respectively, and R^D_{Old} and R^D_{New} as the thermal resistance between the old and new hot face positions and the tip of the shallow thermocouple respectively, the following equations can be derived:

$$T_{HF} = T_{d,f} + H_{flux} \times R^D_{Old} \tag{11}$$

$$T_{HF} = T_{d,m} + H_{flux} \times R^D_{New} \tag{12}$$

$$T_{HF} = T_{s,f} + H_{flux} \times R^S_{Old} \tag{13}$$

$$T_{HF} = T_{s,m} + H_{flux} \times R^S_{New} \tag{14}$$

Solving Eqs. (11)–(14), the thermal resistances, R^D_{New} and R^S_{New}, can be obtained by Eqs. (15) and (16) respectively.

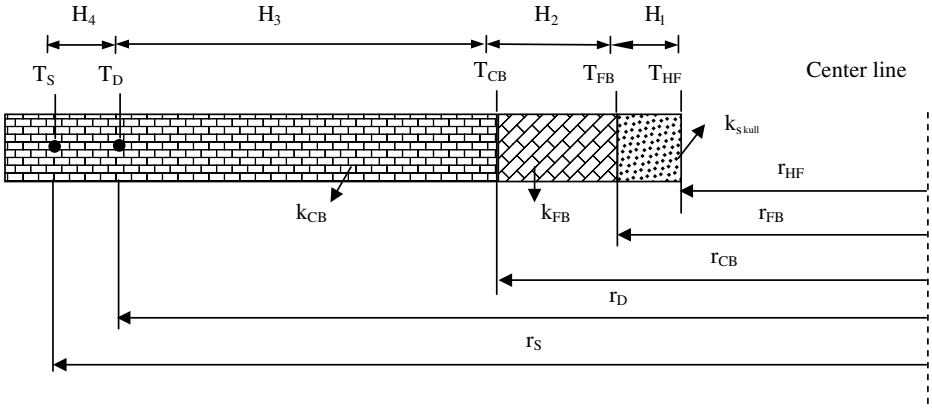

(a) A case with all three layers including carbon block, firebrick and skull

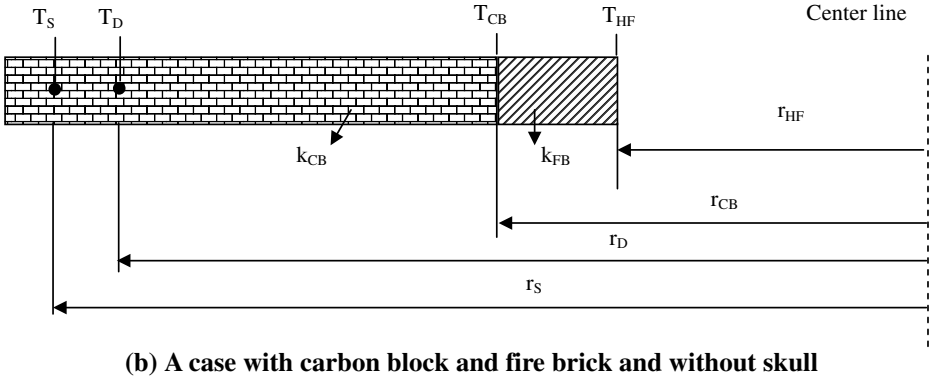

(b) A case with carbon block and fire brick and without skull

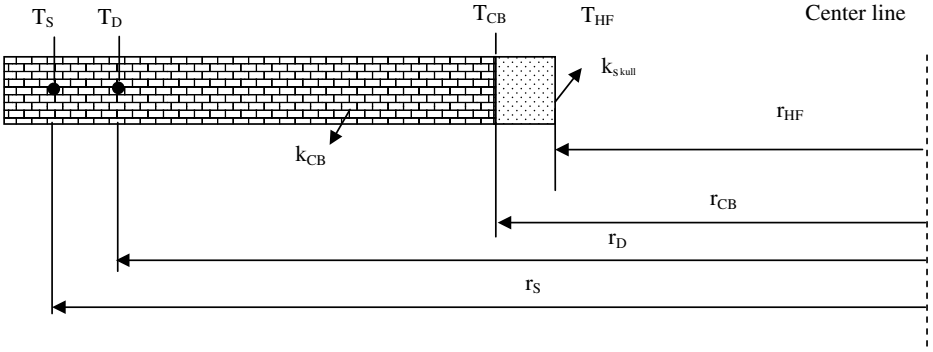

(c) A case with carbon block and skull and without firebrick

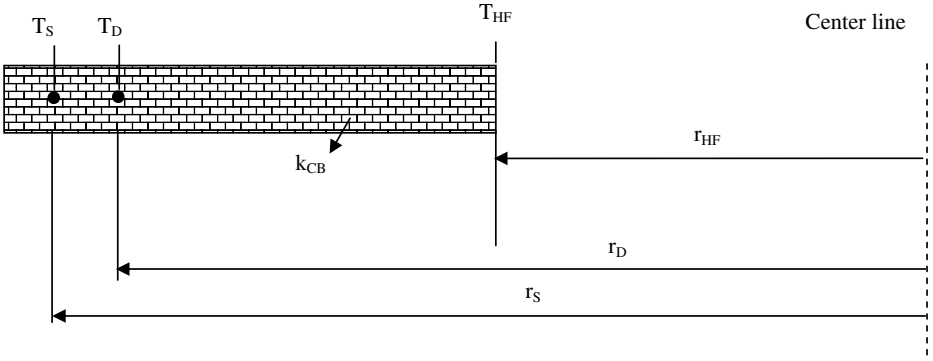

(d) A case with carbon block only

Fig. 4. Side wall structures at different scenarios.

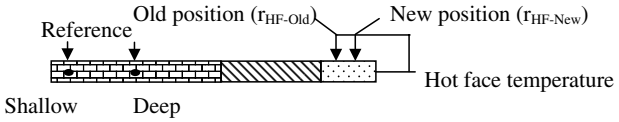

(a) A case with both old and new hot faces are located in skull

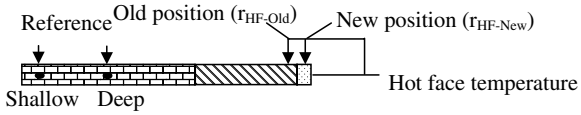

(b) A case with the old hot face in skull and the new hot face in firebrick

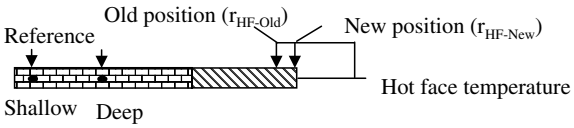

(c) A case with both old and new hot faces in firebrick

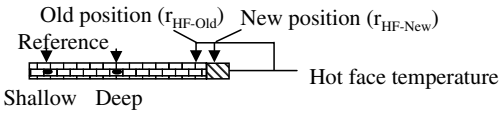

(d) A case with the old hot face in firebrick and the new one in carbon block

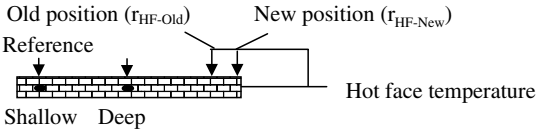

(e) A case with both old and new hot faces in carbon block

Fig. 5. Fine tuning methodology for different situations.

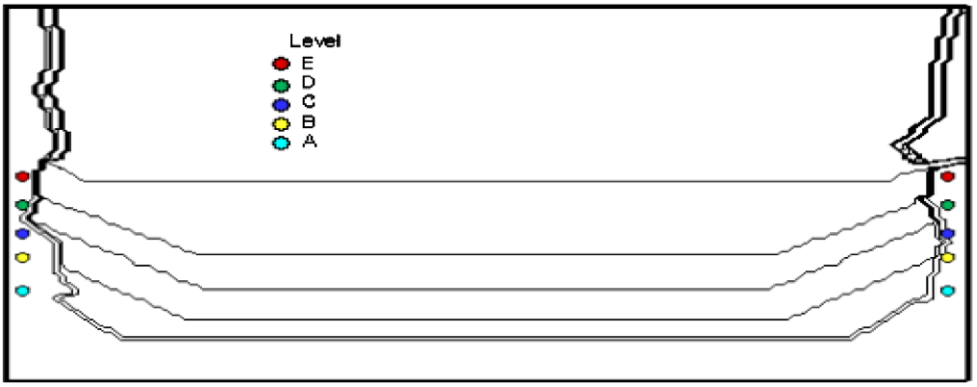

Fig. 6. The inner profile of an blast furnace hearth out of commission.

$$R^{D}_{New} = R^{D}_{Old} + \frac{T_{d,f} - T_{d,m}}{H_{flux}} \quad (15)$$

$$R^{S}_{New} = R^{S}_{Old} + \frac{T_{s,f} - T_{s,m}}{H_{flux}} \quad (16)$$

In the case that the blow-in lining still exists, based on the Eq. (11), the R^{D}_{Old} and R^{D}_{New} can be given as follows, respectively:

$$R^{D}_{Old} = \frac{1}{k_{FB}} \ln\left(\frac{r_{CB}}{r_{HF}}\right) + \frac{1}{k_{CB}} \ln\left(\frac{r_{D}}{r_{CB}}\right) + \frac{1}{k_{skull}} \ln\left(\frac{r_{FB}}{r_{HF\_Old}}\right) \quad (17)$$

and

$$R^{D}_{New} = \frac{1}{k_{FB}} \ln\left(\frac{r_{CB}}{r_{HF}}\right) + \frac{1}{k_{CB}} \ln\left(\frac{r_{D}}{r_{CB}}\right) + \frac{1}{k_{skull}} \ln\left(\frac{r_{FB}}{r_{HF\_New\_D}}\right) \quad (18)$$

Substituting Eqs. (17) and (18) into Eq. (15) and rearranging it, the following equation can be obtained:

$$\frac{T_{d,m}-T_{s,m}}{\frac{1}{K_{CB}}\left(\ln\left(\frac{r_s}{r_d}\right)\right)}=\frac{T_{d,f}-T_{d,m}}{\frac{1}{K_{skull}}\left(\ln\left(\frac{r_{HF\_New\_D}}{r_{HF,old}}\right)\right)} \tag{19}$$

Solving Eq. (19) based on the deep thermocouple, the new hot face radius can be calculated in Eq. (20)

$$r_{HF\_New\_D}=\frac{r_{HF\_Old}}{\exp\left(\frac{K_{skull}}{K_{CB}}\times\ln\left(\frac{r_s}{r_d}\right)\times\frac{T_{d,f}-T_{d,m}}{T_{d,m}-T_{s,m}}\right)} \tag{20}$$

Similarly,

$$R^{S}_{Old}=\frac{1}{k_{FB}}\ln\left(\frac{r_{CB}}{r_{HF}}\right)+\frac{1}{k_{CB}}\ln\left(\frac{r_S}{r_{CB}}\right)+\frac{1}{k_{skull}}\ln\left(\frac{r_{FB}}{r_{HF\_Old}}\right) \tag{21}$$

and

$$R^{S}_{New}=\frac{1}{k_{FB}}\ln\left(\frac{r_{CB}}{r_{HF}}\right)+\frac{1}{k_{CB}}\ln\left(\frac{r_S}{r_{CB}}\right)+\frac{1}{k_{skull}}\ln\left(\frac{r_{FB}}{r_{HF\_New\_S}}\right) \tag{22}$$

Substituting Eqs. (21) and (22) into Eq. (16) and rearranging it, gives

$$\frac{T_{d,m}-T_{s,m}}{\frac{1}{K_{CB}}\left(\ln\left(\frac{r_s}{r_d}\right)\right)}=\frac{T_{s,f}-T_{s,m}}{\frac{1}{K_{skull}}\left(\ln\left(\frac{r_{HF\_New\_S}}{r_{HF,old}}\right)\right)} \tag{23}$$

Solving Eq. (23), the following equation can be obtained.

$$r_{HF\_New\_S}=\frac{r_{HF,old}}{\exp\left(\frac{K_{skull}}{K_{CB}}\times\ln\left(\frac{r_s}{r_d}\right)\times\frac{T_{s,f}-T_{s,m}}{T_{d,m}-T_{s,m}}\right)} \tag{24}$$

The final hot face position can be obtained by averaging Eqs. (20) and (24).

$$r_{HF\_New}=\frac{(r_{HF\_New\_D}+r_{HF\_New\_S})}{2} \tag{25}$$

The fine tuning procedure described above can be applied to local areas which have large differences between the predicted and measured temperatures. This fine tuning procedure can improve the accuracy significantly except for the areas near the corners. Since the heat transfer process is not one-dimensional in the corner areas, additional two-dimensional or three-dimensional fine tuning procedures are needed. A preliminary 2-D fine tuning procedure has been developed. The principle of the 2-D corner tuning is similar to that of 1-D fine tuning. Due to the space limit, the details of this procedure and its further refinement will be presented in the future work.

6. Results and discussion

6.1. Validation of 3-D CFD hearth model

The 3-D CFD model was validated by comparing the calculated and measured flow velocities in a water model [18]. Good agreements have been obtained between CFD results and experimental data [19]. The measurements in a real blast furnace, Mittal IH7, were also used to validate the CFD model. Fig. 6 displays the inner profile of the IH7 blast furnace at its campaign end of 2003, which was measured during the hearth demolishment for the furnace reline. During the operation, there were 5 thermocouple groups which named A, B, C, D, and E respectively embedded in the refractory at different elevations to record refractory temperatures. CFD simulation was conducted using the given inner profile and comparisons were made between the predicted and measured temperatures at the end of the campaign in 2003 as shown in Fig. 7. It illustrates that, since the inner profile of the hearth is accurately known, the CFD predicted temperatures based on this known inner profile matched the thermocouple measured results very well [20].

6.2. Prediction of the inner profile

The methodology presented above has been applied to predict the inner profiles of the new Mittal Steel IH7 Blast Furnace at different time periods after the major relining in October 2003. 298 thermocouples are installed on the side-

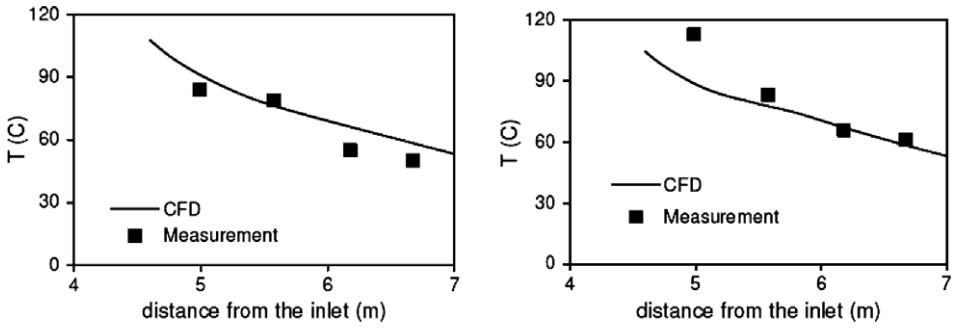

Fig. 7. The comparison between CFD predicted and thermocouple measured.

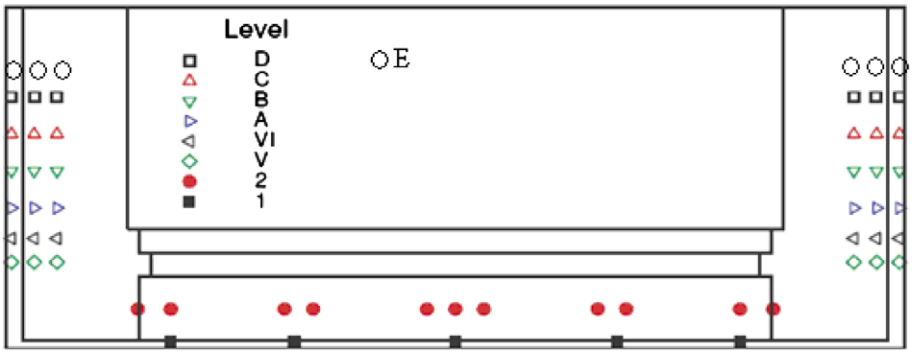

Fig. 8. Locations of thermocouples.

walls and bottom of the hearth at the locations inside the carbon blocks and near the cold faces as shown in Fig. 8.

Figs. 9–12 present the predicted results for the first month of operation after the major relining of the IH7 blast furnace. The prediction of hearth inner profile of IH7 blast furnace after the first month operation was started from the brand new hearth without any erosion and nor skull on the inner face of the hearth, which is called the baseline case with the fresh geometry. A few iterations of simulations were made using the developed methodology to predict the inner profile. Fig. 9 illustrates the average hot face temperature as a function of height for different iterations. It shows that the hot face temperatures do not change and are converged after three iterations. The hot face temperature is non-uniform and decreases from top to bottom along the height due to the heat loss through the side walls. The results suggest that it is important to consider the non-uniform distributions of the hot face temperatures.

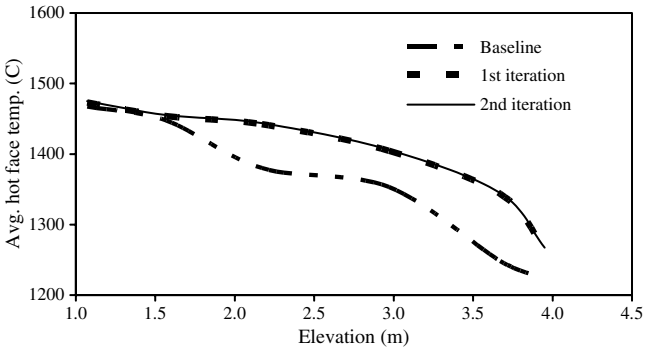

Fig. 9. Average hot face temperatures.

Fig. 10a and b shows the predicted inner profiles after three iterations, which is called case A, and fine tuning, which is called case B, respectively after the first month operation, i.e., at the end of October 2003. In both figures, there is skull formation on both sidewall and bottom of the hearth. The skull thickness in case B (after fine tunings) is thinner than that in case A (after three iterations). The fine tuned regions are highlighted with circles. Figs. 11a–c are the parity plots for the baseline case with fresh geometry and cases A and B. The dots are the comparisons between measured and predicted temperatures at all the thermocouple locations and the dashed line represents a perfect match. If predicted temperatures are greater than measured temperatures, the hearth lining thickness will be under predicted, and vice versa. In the baseline case, the fresh geometry without skull was used in the CFD simulation. Obviously, the predicted temperatures are higher than those in reality, which indicates the skull must have been built up. In case B, the skull is built up but the thickness is overestimated. Therefore, the predicted temperatures are lower than measured ones in many locations. After fine tuning, the skull thickness becomes thinner and the predicted temperatures are more accurate as shown in Fig. 11c. The final inner profile indicates the firebrick still exists and no hearth erosion in the first month of operation of the blast furnace. Table 1 shows examples of the percentage difference between predicted and measured temperatures. Averaged differences for all the thermocouples at three levels (A, B, and C) indicate that the differences

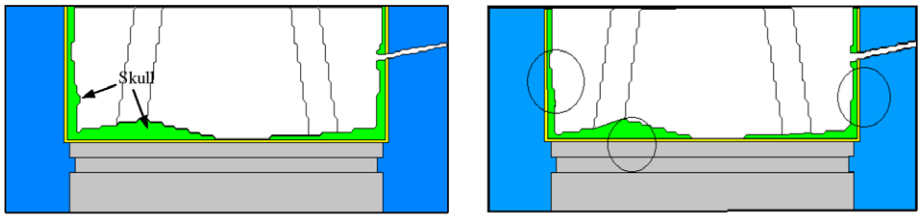

(a) Inner profile after three iterations (b) 3-Inner profile after fine tunings

Fig. 10. Predicted inner profiles at a vertical plane through the taphole in the first month of operation (October 2003).

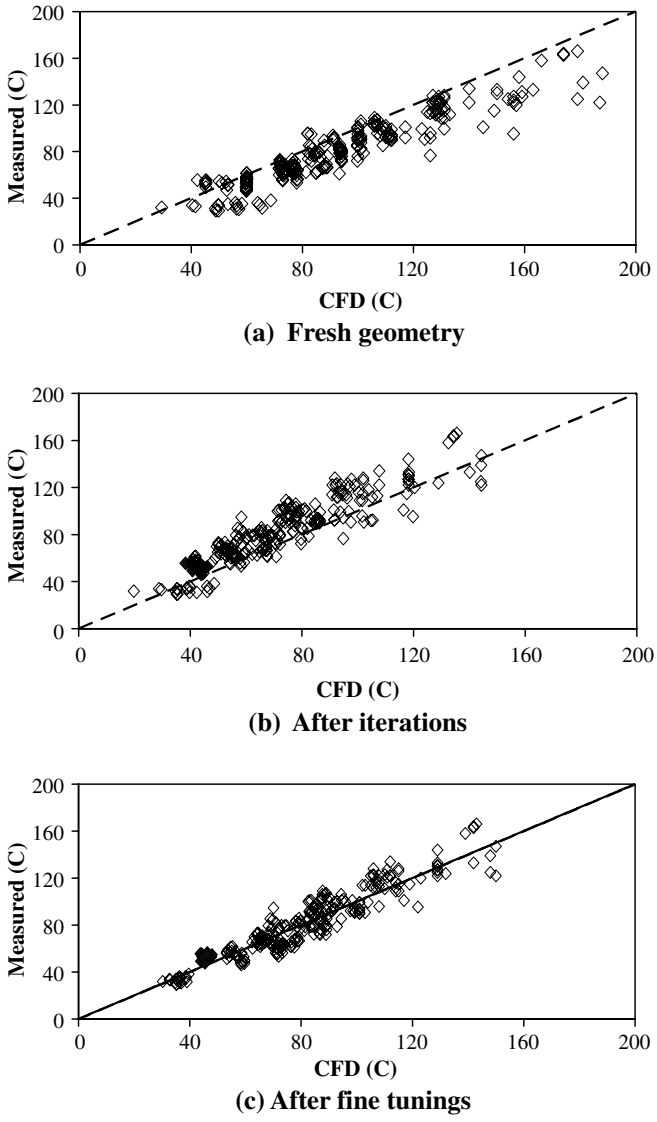

Fig. 11. Comparison be between measured and calculated temperatures.

Table 1
Examples of percentage difference between predicted and measured temperatures at different steps

Thermocouple group	Distance from inlet (m)	Average % difference		
		Baseline case (fresh geometry)	Case A (after three iterations)	Case B (after fine tuning)
Level A	3.67	28.98	16.49	10.52
Level B	2.97	27.76	15.95	8.93
Level C	2.17	26.46	16.13	4.44

significantly reduced in each iteration step. The difference is the largest at level A because it is near the corner region. Although this difference at level A is acceptable, a more efficient method to treat the corner region still needs to be developed in the future fro more accurate predictions. The average percentage difference between predicted and measured temperatures for all the thermocouples is 9.8% after the fine turning.

Figs. 12a and b show the inner profile and velocity vectors in a side and a top view respectively. In the figure, x is along the vertical direction, z is along the horizontal direction toward the tap hole and y is along the horizontal direction perpendicular to x and z directions. The top view displays that the inner profile is truly 3-D in nature and a ring shaped channel flow. Since the center dead zone is not permeable to the fluid, the hot metal is not able to flow through the deadman directly to the taphole and can only travel through more porous zones peripherally. In the side view, the hot metal enters the hearth vertically from the top with a very small velocity. In the regions near the taphole, it is directly drained out and the velocity is relatively large. In contrast, velocities of hot metal flow are very low near the deadman region and at the corner opposite to the taphole.

Figs. 13 and 14 show the finalized predictions of the hearth inner profiles of IH7 blast furnace at the end of December 2003 and January 2004 respectively. It shows that skull is first built up and then melted in most of the regions. At the end of January, the firebrick disappeared and carbon blocks started to be eroded at the side wall near the taphoel level. Although the dead zone is assumed to be sitting on the bottom skull, the ceramic pads bottom

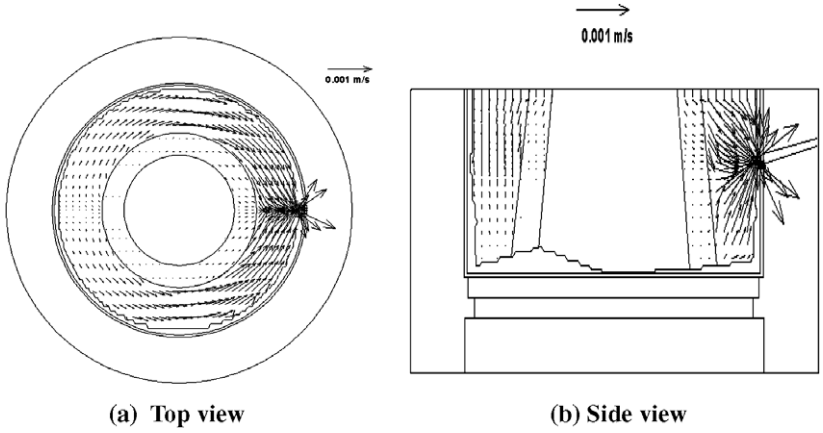

Fig. 12. Inner profile and velocity vectors.

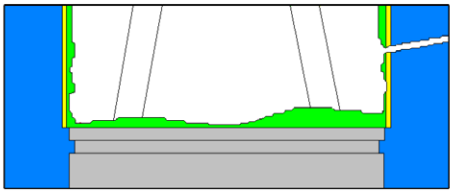

(a) At a vertical plan through taphole

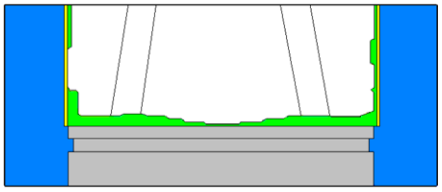

(b) At a vertical plan with 90 degree from taphole

Fig. 13. Predicted inner profile at the end of December, 2003.

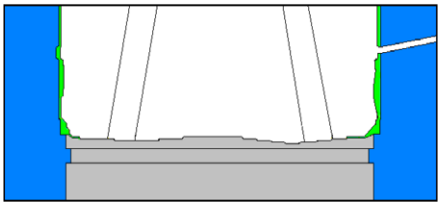

(a) At a vertical plan through taphole

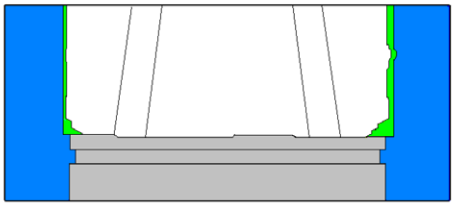

(b) At a vertical plan with 90 degree from taphole

Fig. 14. Predicted inner profile at the end of January, 2004.

seemed to be eroded too. More detailed analysis for the dead zone position needs to be done in the future.

7. Conclusions

A methodology has been developed which integrates the 3-D CFD model and the 1-D heat transfer model to estimate and analyze the erosion and inner profile of a blast furnace hearth. This methodology is computationally efficient and reasonably accurate. It makes possible to predict the hearth erosion and inner profile for real blast furnace in operation. Its application to a real blast furnace showed good agreements between predicted and measured refractory temperatures and displayed the inner hearth profiles at the first few months of operation of a new blast furnace hearth. Simulations will be continued for predicting the inner hearth profile at different operation time periods. More effective fining tuning procedure for the corner areas will be developed.

Acknowledgments

Special thanks to Indiana 21st Century for supporting this research and to Dr. Fang Yan for his contribution to the part of the software development.

References

[1] D. Huang, P. Chaubal, H. Abramowitz, C. Zhou, Hearth Skulls and Hearth Wear Investigation of ISPAT Inland's #7 Blast Furnace, in: AIST 2005 Proceedings, AIST Proceedings, Charlotte, North Carolina, vol. 1, USA, 2005, pp. 101–112.
[2] Johnny Br'annbacka, Henrik Saxen, Novel model for estimation of liquid levels in the blast furnace hearth, Chem. Eng. Sci. 59 (2004) 3423–3432.
[3] W.T. Cheng, C.N. Huang, S.W. Dub, Three dimensional iron flow and heat transfer in the hearth of a blast furnace during tapping process, Chem. Eng. Sci. 1 (60) (2005) 4485–4492.
[4] F. Yoshikawa, J. Szekely, Mechanism of blast furnace hearth erosion, Ironmak. Steelmak 8 (1981) 159–168.
[5] A. Preuer, J. Winter, H. Hiebler, Computation of the erosion in the hearth of a blast furnace, Steel Res. 63 (4) (1992) 147–151.
[6] M. Tachimori, Flow of Iron in Blast Furnace Hearth, Tetsu to Hagane (in Japanese) 70 (1984) 2224–2231.
[7] J. Ohno, M. Tachimori, M. Nakamura, Y. Hara, Influence of hot metal flow on the heat transfer in a blast furnace hearth, Tetsu to Hagane (in Japanese) 71 (1985) 34–40.
[8] K. Shibata, Y. Kimura, M. Shimizu, S. Inaba, Dynamics of dead-man coke and hot metal flow in a blast furnace hearth, ISIJ International 30 (3) (1990) 208–215.
[9] V. Panjkovic, J.S. Truelove, P. Zulli, Numerical modelling of iron flow and heat transfer in blast furnace hearth, Ironmak. Steelmak. 29 (2002) 390–400.
[10] J. Torrkulla, H. Saxen, Model of the state of the blast furnace hearth, ISIJ Int. 40 (5) (2000) 438–447.
[11] J. Torrkulla, J. Brannbacks, H. Saxen, Indicators of the internal state of the blast furnace hearth, ISIJ Int. 42 (5) (2002) 504–511.
[12] K. Takatani, T. Inada, K. Takata, Mathematical model for transient erosion process of blast furnace hearth, ISIJ Int. 41 (10) (2001) 1139–1145.
[13] R. Stokman, E. Stein Callenfels, R. Laar, Blast furnace lining and cooling technology: experiences at Corus Ijmuiden, Iron Steel Technol. (2004) 21–28.
[14] D. (Frank) Huang, Yu Zhang, Rohit Deshpande, Pinakin Chaubal, Chenn Q. Zhou, Simulation of the hearth draining process and thermal stress of a BF hearth, in: AIST Proceedings, Indianapolis, Indiana, USA, 2007.
[15] F. Yan, C.Q. Zhou, D. Huang, P. Chaubal, A. Zhao, 3-D computational modeling of a blast furnace hearth, Iron Steel Technol. 2 (1) (2005) 48–58.
[16] D. Huang, P. Chaubal, F. Yan, C. Zhou, The use of a CFD model for understanding the internal conditions in a blast furnace hearth. in: The 5th European Coke and Ironmaking Congress, Stockholm, Sweden, 2005, pp. 1–15.
[17] Chenn Q. Zhou, Fang Yan, David Roldan, D. (Frank) Huang, Pinakin Chaubal, Yongfu Zhao, Evaluation of internal conditions in a blast furnace hearth using a 3-D CFD model, in: AIST Proceedings, Charlotte, North Carolina, vol. 1, USA, 2005, pp. 284–292.
[18] A.G.A. Nnanna, A. Uludogan, D. Roldan, C.Q. Zhou, P. Chaubal, D. Huang, Water model of a blast furnace for flow pattern investigation, in: AIST Proceedings, Charlotte, North Carolina, vol. 1, USA, 2005, pp. 35–46.

[19] Anil Kumar Patnala,. Numerical investigation on flow characteristics of blast furnace hearth. Master thesis, Purdue University Calumet, USA, 2005.
[20] David Roldan, Numerical investigation of the erosion in a blast furnace hearth, Master thesis, Purdue University Calumet, USA, 2005.
[21] Cheng-Hung Huang, Hung-Chi Lo, A three-dimensional inverse problem in predicting the heat fluxes distribution in the cutting tools, Numer. Heat Transfer 48 (10) (2005) 1009–1034.
[22] R.G. Hills, E.C. Hensel Jr., One-dimensional nonlinear inverse heat conduction technique, Numer. Heat Transfer 10 (4) (1986) 369–393.
[23] Weizhong Dai, Zongwen Fen, Raja Nassar, James Palmer, A combined analytic and numerical method for predicting the solid-layer growth from melt crystallization, Numer. Heat Transfer 44 (6) (2003) 577–590.